Passivity-based control incorporating trajectory planning for a variable-reluctance finger gripper

J M Yang[1], **X Jin**[1]*, **J Wu**[1], **N C Cheung**[2] and **K K-C Chan**[2]
[1]Electric Power College, South China University of Technology, Guangzhou, People's Republic of China
[2]Hong Kong Polytechnic University, Hung Hom, Hong Kong

Abstract: A novel two-finger gripper using variable-reluctance (VR) technology is investigated in this paper. Its non-linear characteristics are explored through theoretical analysis and experiments. Based on the experimental model, a passivity-based controller is designed. With energy modification and damping injection, the robustness to variable inductance is verified by simulations and experiments. Through the incorporation of passivity-based control (PBC) with differential flatness, trajectory planning is realized and ideal performance is achieved.

Keywords: finger gripper, variable reluctance, passivity-based control, differential flatness

NOTATION

$\boldsymbol{e}_d$	state error
$\boldsymbol{g}$	input voltage vector
$H(\boldsymbol{x})$	total energy function
i	stator current, coil current
J_m	total rotor and load inertia
$\mathbf{J}(\boldsymbol{x})$	skew-symmetric matrix
K_{sp}	spring constant
K_v	viscous damping constant
K'	constant
$L(\theta)$	coil self-inductance
$L'(\theta)$	leakage inductance
$\mathbf{R}$	matrix
R_m	stator winding resistance
u	input voltage
$\boldsymbol{x}$	state vector
$\boldsymbol{x}_d$	reference state vector
θ	angular position
λ	flux linkage
λ'	leakage flux linkage
$\boldsymbol{\xi}$	disturbance vector

The MS was received on 12 August 2003 and was accepted after revision for publication on 25 September 2003.
* *Corresponding author: Computer Science Department, University of Manchester, IT Building IT301, Oxford Road, Manchester M13 9PL, UK.*

1 INTRODUCTION

The gripper mechanism plays an important role in factory automation, robotics and industry applications. Various gripper machine configurations have been explored. Actuators ranging from traditional d.c. motors and voice coils to thermal and pneumatic actuators are employed. Recently, electrostatic, piezoelectric and switched reluctance grippers have also been designed to broaden the scope [**1**–**5**].

The manipulator directly based upon the principle of the variable-reluctance motor (VRM) has drawn much research attention over the past decade owing to its robust, low-cost structure and its potential for numerous industrial applications. However, since the VRM has inherited non-linear characteristics, problems involved with torque ripple and non-uniform force occur when it is driven by standard motor drives. Over the past few years, many publications on VRM designs, commutation methods and VRM drives have emerged. These methods were made feasible with the advancement of non-linear control theory, power electronic techniques and computer processing power [**6**]. Now, it is worth considering putting most of the non-linear side-effects into the construction and simulation of the VRM model, as well as real-time control of the VRM hardware.

Applying a VRM manipulator to driving the gripper is a virtual method. It was first introduced by Ilic'-Spong *et al.* [**7**]. They carried out exact linearization controls based on the theory of differential geometry and specific commutation methods. Although the designed linearization controller can set up the phase current before the

previous phase current has attenuated, this control strategy has distinct disadvantages, such as its computation relying on the exact parameters of the plant model. Therefore, it is not robust enough to the variation in plant parameters. To overcome this defect, an adaptive technique is adopted. Amor and Dessaint designed another controller for the VRM manipulator by combining the exact linearization and adaptive techniques [**8**]. Amor and Dessaint's controller has finite robustness to parameter variation but neglects the non-linear characteristics of the VR so that its results are different from the characteristics of a virtual manipulator. Considering the VRM in a low-velocity, high-torque mode of operation, Bortoff, Kohan and Milman presented an adaptive controller based on the full-state feedback and observer [**9**]. The 'torque sharing function' is adopted to smooth commutation among phases and to increase the peak torque available from the motor.

In the methods mentioned above, for the control strategies of the VR manipulator it is assumed that its parameters are known exactly or the unknown parameters can be identified by the adaptive technique. However, the parameters of the VR manipulator are not exactly known and always vary with current and position. Actually, control is difficult to implement owing to its complex algorithm when considering the structural information of VR in design. Improving the applicability of the VR gripper on the basis of the simplified model and taking the structural characteristics into account is a significant step in designing the controller of the VR gripper.

In this paper, a non-linear feedback controller, which effectively combines the natural energy dissipation properties of the VR gripper system with its differential flatness property [**10**, **11**], is proposed. These two important structural properties of the system can be combined in the context of a dynamic passivity based feedback controller. The proposed controller arises from the consideration of 'energy modification and damping injection', which is achievable through identifying and exploiting the natural 'conservative and dissipation' structure of the non-linear system dynamics and taking advantage of the hidden linear controllable features of the system, represented by the flat output.

A gripper requires different response speed during the operation phase. During the off-duty period, the speed should be high to increase the efficiency. On start-up and with the workpiece adjacent, the speed should be low to avoid impact with the mechanism. If the trajectory planning is aimed at the coil current, it is hard to avoid torque ripple. Therefore, the dynamic system can be regarded as an energy transform system. If the trajectory planning is aimed at the energy injected into the coil, flat response of the rational angle is predictable.

In reference [**12**], assuming that a model of the ordinary VRM is exactly linearized by the state feedback, the system possesses a structural property known as differential flatness. A globally stable controller is designed by passivity-based control (PBC), and a desired trajectory for the coil current is planned by differential flatness. Roughly speaking, a system is flat if there exist certain special outputs, called flat outputs, equal in number to the inputs, that are functions of the state and a finite number of its time derivatives. In addition, every variable in the system (states, outputs, control inputs) can, in turn, be expressed as functions of the flat outputs and a finite number of their time derivatives. Differential flatness is a remarkable structural property of the system that enables connections to be established between all properties important to the system with a particular feedback control design methodology. Differential flatness has been successfully applied in solving trajectory planning problems of complex multivariable non-linear systems [**13**, **14**].

Section 2 presents a simple analysis of the VR structure and model. The energy shaping plus damping injection based dynamic feedback controller is presented in section 3. In addition, the required performance and robustness are implemented by VR energy shaping and damping injection. In section 4, the current trajectory planning is implemented for flat rotational angle dynamics. The effects of combining the passivity-based control with trajectory planning are explored by simulations and experiments. The experimental implementation and its results are shown in section 5.

2 PROPOSED STRUCTURE AND MODEL OF THE VR GRIPPER

2.1 Structure and flux profile

The structure of the two-finger VR gripper is shown in Fig. 1. It consists of two rotary elements, each attached to a finger. The stator contains two coils, each with a 400-turn winding. The moving rotors are mounted onto two individual shafts, the axes of which are normal to the plane of the diagram. The moving elements may rotate freely between the poles of the stator. Both the rotors and stators are made up of laminated mild steel to reduce eddy currents.

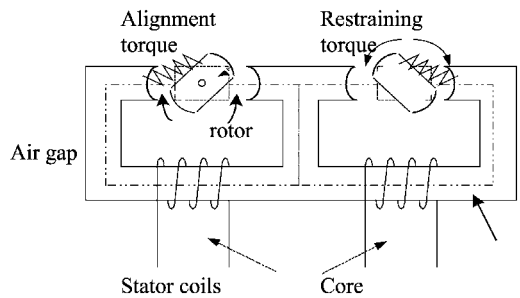

Fig. 1 Structure block of the variable-reluctance finger gripper

The two fingers of the gripper are 90 mm long and spring loaded. This arrangement allows bidirectional movement from a single-direction coil excitation. When currents are applied to the stator windings, the rotors will rotate away from initial rest positions with a tendency to reduce their reluctance by torque alignment. When the fingers rotate by 70°, the fingertips will be fully closed. Incremental rotary encoders with a resolution of 0.09° are mounted onto the actuator shafts to measure the rotor positions. The flux characteristics in different situations acquired from experiments are shown in Fig. 2.

The overall construction is extremely simple and robust, and very similar to the rotary solenoids using simple on–off mechanical actuation devices. Combining the two fingers into a single magnetic housing has made the finger alignment process much simpler and the overall size much smaller.

Assume that the flux can be expressed as

$$\lambda = L(\theta)i$$

where λ is the self-flux linkage, $L(\theta)$ is the coil self-inductance and i is the coil current.

Because the structure of the VR gripper is open, the leakage flux linkage cannot be neglected. It is assumed that the leakage flux linkage takes the form of a self-inductance linkage, i.e.

$$\lambda' = L'(\theta)i$$

where λ' is the leakage flux linkage and $L'(\theta)$ is the leakage inductance.

The state dynamic equation of the VR finger gripper can be represented as

$$J_m\ddot{\theta} = -K_{sp}\theta - K_v\dot{\theta} + i\frac{\partial\lambda}{\partial\theta} \tag{1}$$

where J_m is the total rotor and load inertia, θ is the angular position of the rotor, K_{sp} is the spring constant, K_v is the viscous damping constant, i is the stator current and λ is the flux linkage.

Then, the following equation can be achieved:

$$(L + L')\dot{i} = \boldsymbol{u} - \left(R_m i + \frac{\partial\lambda}{\partial\theta}\dot{\theta}\right) \tag{2}$$

where $\boldsymbol{u}$ is the input voltage across the stator winding and R_m is the stator winding resistance.

2.2 Port-controlled Hamiltonian model

The state vector, $\boldsymbol{x}$, is selected as

$$\boldsymbol{x} = [Li \quad K_{sp}\theta \quad J_m\dot{\theta}]^T$$

The total energy function, $H(\boldsymbol{x})$, can be defined as the sum of electromagnetic stored energy and kinetic energy and stored spring potential energy:

$$H(\boldsymbol{x}) = \tfrac{1}{2}(Li^2 + K_{sp}\theta^2 + J_m\dot{\theta}^2) \tag{3}$$

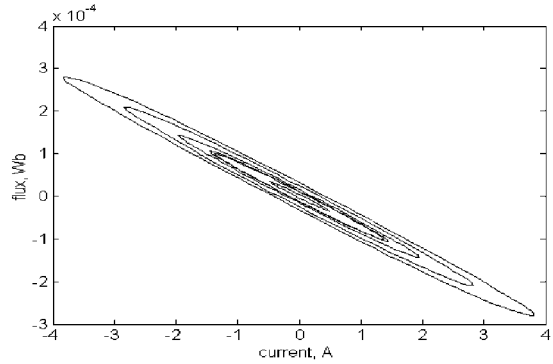

Self-flux characteristics to different current

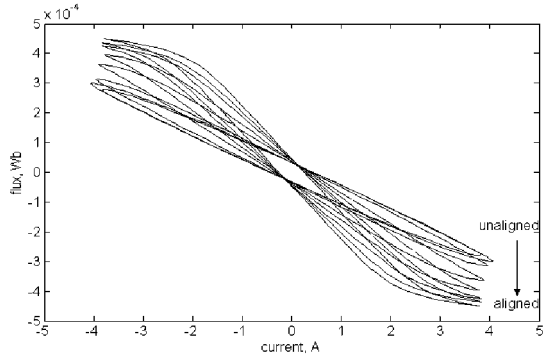

Self-flux characteristics to different angle

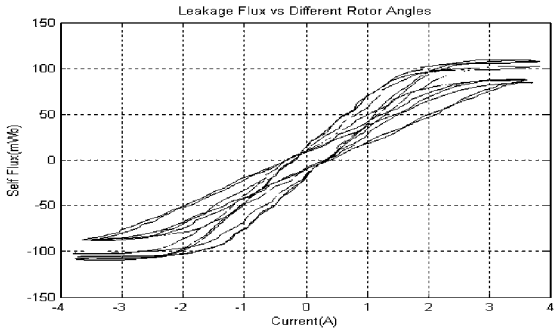

Leakage Flux linkage versus different rotor positions

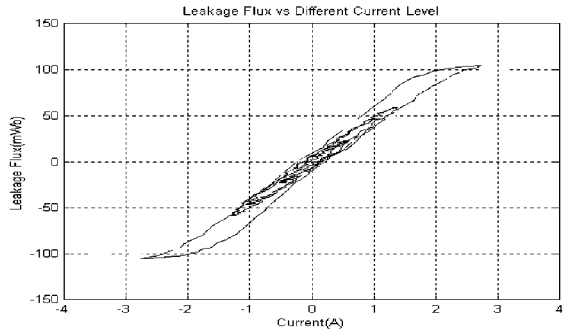

Leakage Flux linkage versus different current level

Fig. 2 Flux characteristics in different situations

With this energy function, the model of the VR finger gripper stated in equations (1) and (2) can be rearranged as the formula of the port-controlled Hamiltonian (PCH):

$$\dot{\boldsymbol{x}} = [\mathbf{J}(\boldsymbol{x}) - \mathbf{R}] \cdot \frac{\partial H(\boldsymbol{x})}{\partial \boldsymbol{x}} + \boldsymbol{g} \cdot \boldsymbol{u} + \boldsymbol{\xi} \tag{4}$$

where $\mathbf{J}(\boldsymbol{x})$ is a skew-symmetric matrix, $\mathbf{R}$ is a semi-positive definite matrix, $\boldsymbol{g}$ is the input voltage vector and $\boldsymbol{\xi}$ is the disturbance vector.

It is interesting to note that $\mathbf{R}$, representing dissipative elements, must be positive definite, otherwise the energy stored within the system would not be less than the energy supplied to it and the system would not be a passivity system. Using equations (1) and (2) and the selected state vector $\boldsymbol{x}$ mentioned above, the dynamic model in PCH format can be represented as

$$\dot{\boldsymbol{x}} = \left(\begin{bmatrix} \mathbf{0} & \mathbf{0} & -\dfrac{\mathrm{d}\lambda}{\mathrm{d}\theta} \\ \mathbf{0} & \mathbf{0} & K_{\mathrm{sp}} \\ \dfrac{\mathrm{d}\lambda}{\mathrm{d}\theta} & -K_{\mathrm{sp}} & 0 \end{bmatrix} - \begin{bmatrix} R_{\mathrm{m}} & 0 & 0 \\ 0 & 0 & 0 \\ 0 & 0 & K_{\mathrm{v}} \end{bmatrix} \right) \mathbf{D}^{-1} \boldsymbol{x} + \begin{bmatrix} -\dfrac{\mathrm{d}L'}{\mathrm{d}\theta} \dfrac{x_3}{J_{\mathrm{m}}} \\ 0 \\ 0 \end{bmatrix} \boldsymbol{u} \tag{5}$$

where

$$\mathbf{D} = \begin{bmatrix} (L + L') & 0 & 0 \\ 0 & K_{\mathrm{sp}} & 0 \\ 0 & 0 & J_{\mathrm{m}} \end{bmatrix}$$

The matrix

$$\mathbf{R} = \begin{bmatrix} R_{\mathrm{m}} & 0 & 0 \\ 0 & 0 & 0 \\ 0 & 0 & K_{\mathrm{v}} \end{bmatrix}$$

is a semi-positive definite matrix. The matrix

$$\mathbf{B}(\boldsymbol{x}) = \begin{bmatrix} \mathbf{0} & \mathbf{0} & -\dfrac{\mathrm{d}\lambda}{\mathrm{d}\theta} \\ \mathbf{0} & \mathbf{0} & K_{\mathrm{sp}} \\ \dfrac{\mathrm{d}\lambda}{\mathrm{d}\theta} & -K_{\mathrm{sp}} & 0 \end{bmatrix}$$

is a skew-symmetric matrix ($\boldsymbol{x}^{\mathrm{T}} \mathbf{B} \boldsymbol{x} = 0$). Select the output as

$$y = \frac{x_1}{L + L'}$$

and the input as

$$v = u - \frac{\mathrm{d}L'}{\mathrm{d}\theta} \frac{x_3}{\mathbf{J}} > 0$$

System (5) is passive [**10**]. The variation in self-inductance with position does not destroy the skew-symmetry of the matrix $\mathbf{B}(\boldsymbol{x})$. Therefore, the variation in self-inductance does not influence the stability of the system. The affixation part

$$u' = \frac{\mathrm{d}L'}{\mathrm{d}\theta} \frac{x_3}{\mathbf{J}}$$

in the control signal u is regarded as the compensation current signal to the leakage phenomenon.

In order to ensure convergence of the rational angle, matrix $\mathbf{R}$ should be positive definite. The semi-positive definite matrix $\mathbf{R}$ can be transformed into a positive definite matrix by energy reshaping, as in equation (6). In equation (6), K is a positive number and artificially inserted to maintain the positive definiteness of $\mathbf{R}$. However, with the natural dissipative elements of the actual plant, system damping is small and hence reduces the closed-loop system performance. Additional damping injection is required and is realized by inserting an additional constant, K', into the dissipative matrix $\mathbf{R}$:

$$\dot{\boldsymbol{x}} = \left\{ \begin{bmatrix} 0 & 0 & -\dfrac{\partial \lambda}{\partial \theta} \\ 0 & 0 & K_{\mathrm{sp}} \\ \dfrac{\partial \lambda}{\partial \theta} & -K_{\mathrm{sp}} & 0 \end{bmatrix} - \begin{bmatrix} \mathbf{R} & 0 & 0 \\ 0 & K & 0 \\ 0 & 0 & K_{\mathrm{v}} + K' \end{bmatrix} \right\} \mathbf{D}^{-1} \boldsymbol{x} + \begin{bmatrix} -\dfrac{\mathrm{d}L'}{\mathrm{d}\theta} \dfrac{x_3}{J_{\mathrm{m}}} \\ \dfrac{K}{K_{\mathrm{sp}}} x_2 \\ \dfrac{K'}{J_{\mathrm{m}}} x_3 \end{bmatrix} + \begin{bmatrix} 1 \\ 0 \\ 0 \end{bmatrix} u \tag{6}$$

3 PASSIVITY-BASED CONTROLLER DESIGN

Define the state error as

$$\boldsymbol{e} = \boldsymbol{x} - \boldsymbol{x}_{\mathrm{d}}$$

where $\boldsymbol{x}_{\mathrm{d}}$ is the reference state vector, which defines the desired system performance. Substituting $\boldsymbol{e} = \boldsymbol{x} - \boldsymbol{x}_{\mathrm{d}}$ into equation (6) yields the model of the state error as

$$\dot{\boldsymbol{e}} + [\mathbf{R} - \mathbf{J}] \mathbf{D}^{-1} \boldsymbol{e} = \Phi \tag{7}$$

where

$$\Phi = -\dot{\boldsymbol{x}}_{\mathrm{d}} + [\mathbf{J} - \mathbf{R}] \mathbf{D}^{-1} \boldsymbol{x}_{\mathrm{d}} + \boldsymbol{g} u + \xi$$

The Lyapunov function can be defined as

$$V = \tfrac{1}{2} \boldsymbol{e}^{\mathrm{T}} \mathbf{D}^{-1} \boldsymbol{e} \tag{8}$$

Differentiating $V(\boldsymbol{x})$ to time along the error dynamic system (7) yields the equation

$$\begin{aligned}\dot{V} &= \boldsymbol{e}^{\mathrm{T}}\mathbf{D}^{-1}\dot{\boldsymbol{e}} \\ &= \boldsymbol{e}^{\mathrm{T}}\mathbf{D}^{-1}[(\mathbf{J}-\mathbf{R})\mathbf{D}^{-1}\boldsymbol{e}+\Phi] \\ &= \boldsymbol{e}^{\mathrm{T}}\mathbf{D}^{-1}\mathbf{J}\mathbf{D}^{-1}\boldsymbol{e}-\boldsymbol{e}^{\mathrm{T}}\mathbf{D}^{-1}\mathbf{R}\mathbf{D}^{-1}\boldsymbol{e}+\boldsymbol{e}^{\mathrm{T}}\mathbf{D}^{-1}\Phi \end{aligned} \tag{9}$$

From equation (9), the term $\boldsymbol{e}^{\mathrm{T}}\mathbf{D}^{-1}\mathbf{J}\mathbf{D}^{-1}\boldsymbol{e}$ consists of a matrix $\mathbf{J}$ that is skew symmetric and obviously becomes zero. It has no effect on stability and is known as the workless force. The second term, $-\boldsymbol{e}^{\mathrm{T}}\mathbf{D}^{-1}\mathbf{R}\mathbf{D}^{-1}\boldsymbol{e}$, has matrix $\mathbf{R}$ and $\mathbf{D}^{-1}$, which are both positive definite and make the entire term negative. As long as the term $\Phi = 0$ through suitable control, $\dot{V} \leqslant -\boldsymbol{e}^{\mathrm{T}}\mathbf{R}\boldsymbol{e}$, which ensures the asymptotic convergence of errors.

In order to keep $\Phi = 0$, the reference state needs to comply with the following rules:

1. The rule

$$x_{\mathrm{d}1} = \sqrt{\frac{K_{\mathrm{sp}}\theta^*}{(\mathrm{d}L/\mathrm{d}\theta)^*}} \tag{10}$$

   where $\theta^* = 70^\circ$ and $(\mathrm{d}L/\mathrm{d}\theta)^*$ is the differentiation of self-inductance to angle at time $\theta^* = 70^\circ$.

2. The rule

$$\begin{aligned}&\ddot{x}_{\mathrm{d}2} + \left(\frac{K}{K_{\mathrm{sp}}} + \frac{K_{\mathrm{v}}+K'}{\mathbf{J}}\right)\dot{x}_{\mathrm{d}2} + \left(\frac{K_{\mathrm{sp}}}{\mathbf{J}} + \frac{K_{\mathrm{v}}+K'}{\mathbf{J}}\frac{K}{K_{\mathrm{sp}}}\right)x_{\mathrm{d}2} \\ &= \frac{K}{K_{\mathrm{sp}}}\dot{x}_2 + \frac{K_{\mathrm{sp}}}{\mathbf{J}}\frac{i}{L}\frac{\partial L}{\partial\theta}x_{\mathrm{d}1} + \frac{K_{\mathrm{v}}+K'}{\mathbf{J}}\frac{K}{K_{\mathrm{sp}}}x_2 + \frac{K_{\mathrm{sp}}}{\mathbf{J}}\frac{K'}{\mathbf{J}}x_3 \end{aligned} \tag{11}$$

   where the parameters K and K' are designed so that the state $x_{\mathrm{d}2}$ possesses the required performance. In this context, K and K' are selected as 6 and 1 respectively. This arrangement provides the second-order dynamics of $x_{\mathrm{d}2}$ with the damping ratio $\xi = 0.707$ and the bandwidth $\omega = 700$ rad/s.

3. The control law is designed as

$$\boldsymbol{u} = \frac{r}{L}x_{\mathrm{d}1} + \frac{1}{\mathbf{J}L}\frac{\mathrm{d}L}{\mathrm{d}\theta}x_{\mathrm{d}3}x_1 \tag{12}$$

4 TRAJECTORY PLANNING

The gripper moves at different speeds during the various phases. Besides the effect of state feedback control, the performance of the gripper can also be improved by suitable trajectory planning. The kinetic performance of the gripper is manipulated by the current of the winding which, in turn, is controlled by the voltage imposed on the winding. If the trajectory planning is aimed at the current, fluctuation in speed is unavoidable. The gripper system can be seen as an energy transform system. Its performance is influenced by the energy injected into it. The trajectory planning is made for the energy. A smooth response of the angle is expected.

Table 1 Parameters of grippers

	Notation	Values
Rotor inertia	J_{m}	0.1 mN m
Spring constant	K_{sp}	0.011 N m/rad
Viscous constant	K_{v}	1×10^{-3} N m/rad s
Resistance of stator winding	R_{m}	4 Ω
Number of turns in stator winding	N	400 turns
Maximum continuous current	I	4 A

Define the flat output as

$$F = \tfrac{1}{2}Li^2 \tag{13}$$

Therefore, the current can be expressed in terms of the flat output as

$$i = \sqrt{\frac{2F}{L}} \tag{14}$$

The proposed trajectory guarantees the following initial and terminal conditions:

$$\begin{aligned}&F^*(t_1) = \bar{F}_1, \qquad F^*(t_2) = \bar{F}_2 \\ &\dot{F}^*(t_1) = 0, \qquad \dot{F}^*(t_2) = 0 \\ &\ddot{F}^*(t_1) = 0, \qquad \ddot{F}^*(t_2) = 0 \\ &\frac{\mathrm{d}^3}{\mathrm{d}t^3}F^*(t_1) = 0, \qquad \frac{\mathrm{d}^4}{\mathrm{d}t^4}F^*(t_1) = 0 \end{aligned}$$

According to the operation requirements, as well as the initial and terminal conditions, the flat output is planned as follows:

$$\begin{aligned}F^*(t) = \bar{F}_1 + \Bigg[&21\left(\frac{t-t_1}{\Delta t}\right)^5 - 35\left(\frac{t-t_1}{\Delta t}\right)^6 \\ &+ 15\left(\frac{t-t_1}{\Delta t}\right)^7\Bigg](\bar{F}_2 - \bar{F}_1)\end{aligned} \tag{15}$$

Based on the flat output planning, the trajectory of the reference state, $x_{\mathrm{d}1}$, is planned as

$$x_{\mathrm{d}1} = \begin{cases} 0, & t \leqslant t_1 \\ \sqrt{2LF^*}, & t_1 < t \leqslant t_2 \\ \sqrt{\dfrac{K_{\mathrm{sp}}\theta^*}{(\mathrm{d}L/\mathrm{d}\theta)^*}}, & t > t_2 \end{cases} \tag{16}$$

5 SIMULATIONS AND EXPERIMENTS

The parameters of the grippers in the present study are shown in Table 1.

5.1 Simulations of the PBC for VR grippers

Note that the experiments will be implemented on the DSPACE system (section 5.2). Certain simulation

settings need to be matched with the actual hardware so as to obtain accurate simulation results. The simulation of the passivity-based controller is implemented by using MATLAB SIMULINK. The controller needs to be, on the one hand, fast in dynamics, but, on the other hand, robust enough to stay stable within the entire range of load variation. Slight oscillation can be amplified mechanically and exhibited at the fingertip, adversely affecting the entire system performance. Thus, a 5 kHz sampling rate is selected. In addition, in order to solve differential equations, DSPACE employs an integration solver of the Euler numerical method. The same method is selected for the simulation process.

In the simulation, a step input of 15 mWb with a period of 1 s and an 80 per cent duty cycle is injected into the simulation model. Figure 3 shows that all states have fast tracking responses. The peak time of x_1 is 30 ms, and negligible difference can be found in x_2 and x_3 and their respective desired values.

5.2 Experimental results of PBC plus trajectory planning for the VR gripper

The prototype of the VR finger gripper is shown in Fig. 4. A basic block diagram for the experimental implementation is shown in Fig. 5. The switching power stage converts controlled pulse width modulation

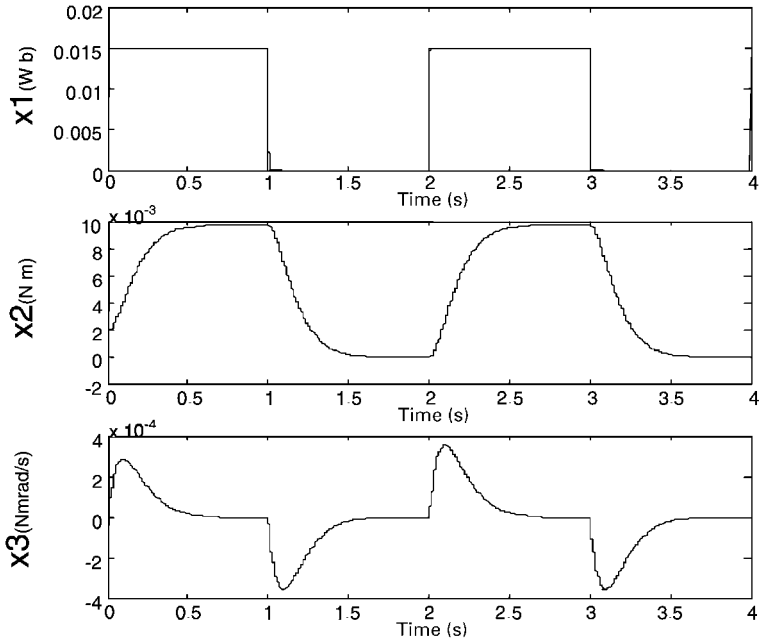

Fig. 3 Simulation results for the tracking responses of each state

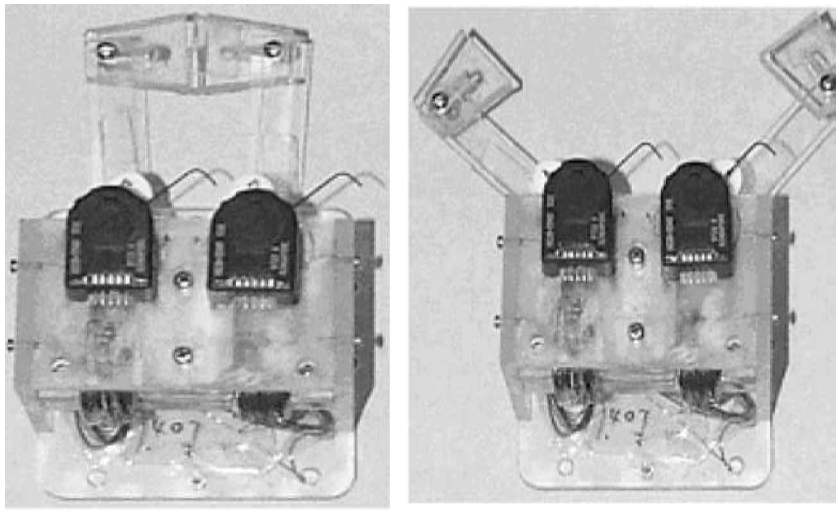

(a) at grasp position (b) at release position

Fig. 4 VR finger gripper

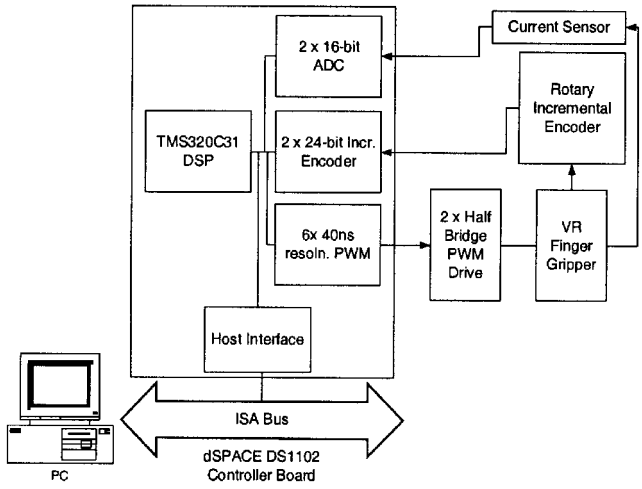

Fig. 5 PBC controller implementation set-up

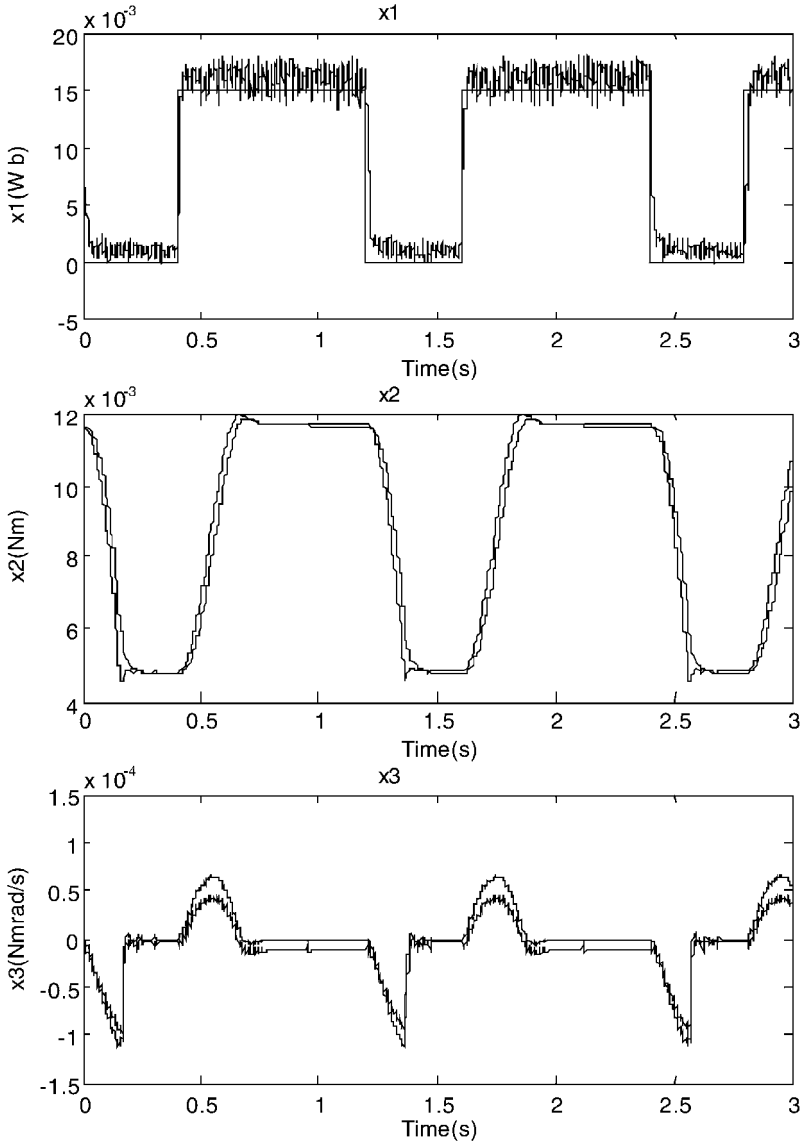

Fig. 6 Experimental results of PBC for the tracking responses of each state

(PWM) signals into a PWM high-voltage source and excites the stator coils. The conditioned current signal and encoder position is sampled by the controller for calculation of the next controlled signal.

The PWM driver used in this project consists of a pair of high–low side power MOSFET, IRF740, half-bridge amplifiers. The driver acts as a current amplifier for the motor. It has fewer components than a full-bridge amplifier and has a true ground which makes current measurement much simpler. The current feedback circuit has a gain of 1.2 A/V. The motor side and logic side are electrically isolated by optocouplers, which may introduce about 300 nS delay. Dead-time delay protection against cross-conduction of the high–low side MOSFETs is introduced. The chopping frequency is set at 24 kHz to ensure good current dynamics and minimal current ripple.

Experimental results of PBC for the VR gripper can be seen in Figs 6 and 7. As expected from the simulation, all states are stable and exhibit high-performance tracking. The noise induced in the x_1 state is mainly due to the switching noise of the current amplifier, whereas the ripple shown in the x_3 state is due to the quantitization error of the encoder.

The damping of the original system is small. Overshooting appears in the tracking of the state x_2. Damping injection can improve the performance. The experimental results of PBC with damping injection are shown in Figs 8 and 9. From Figs 8 and 9 it can be seen that, owing to the damping compensation in the current, the process is smooth.

Figure 10 shows experimental results of the passivity-based control combined with trajectory planning. It is

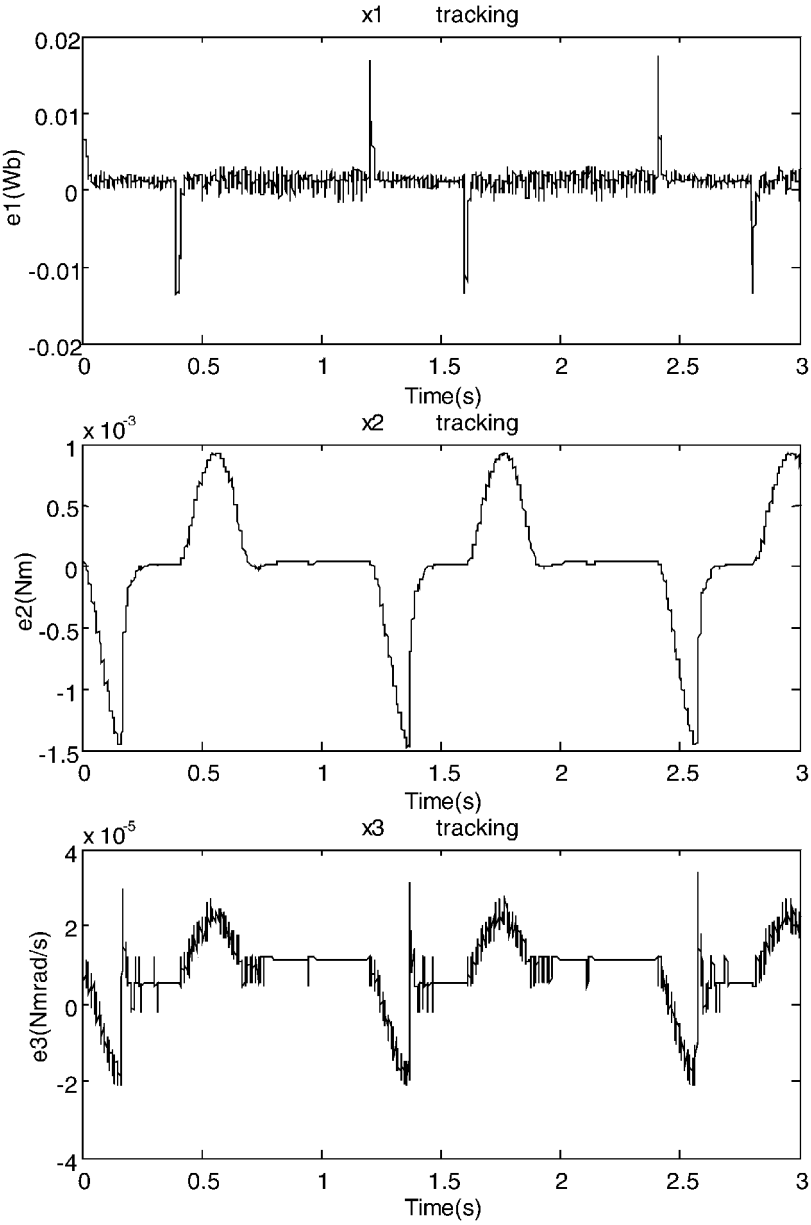

Fig. 7 Experimental results for the tracking error of each state

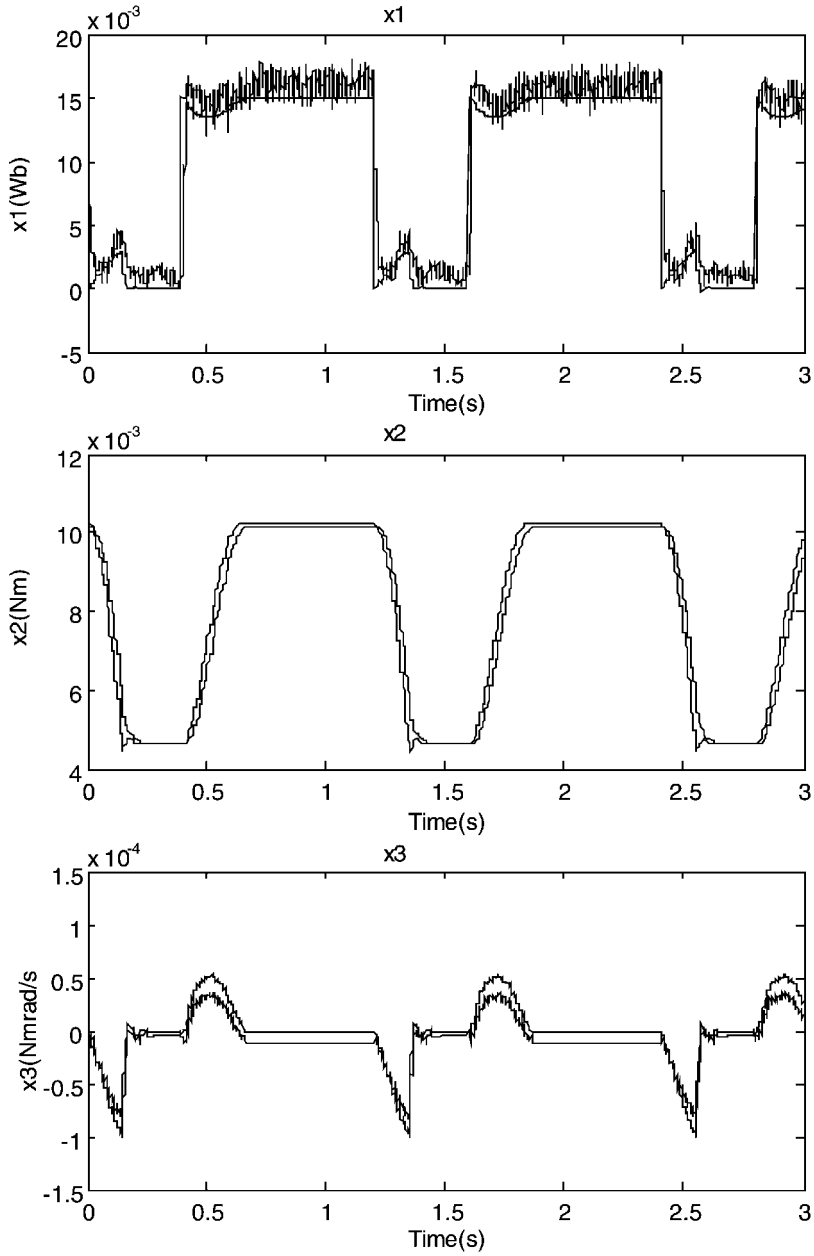

Fig. 8 Experimental results of PBC for the tracking responses of each state with damping injection

obvious that this control strategy makes the gripper operate more smoothly than the previous strategies.

6 CONCLUSIONS

This paper describes controller design, simulation and experimental implementation of the passivity-based plus trajectory planning controller for flux regulation of a variable-reluctance finger gripper.

The passivity-based control strategy guarantees global stability and convergence of the state errors. This controller is robust to variation in the self-flux owing to the structural characteristics of the VR gripper. The performance of the gripper is improved by the design of control parameters. Simulations and experiments demonstrate the effectiveness of the passivity-based controller in regulating the VR finger gripper. By combining PBC with trajectory planning based on differential flatness, the energy trajectory injected into the winding current loop is analysed and planned. Finally, the transition between different operating conditions during different phases of the gripper is implemented flatly.

ACKNOWLEDGEMENTS

The authors would like to acknowledge the funding support from the National Nature Science Foundation of

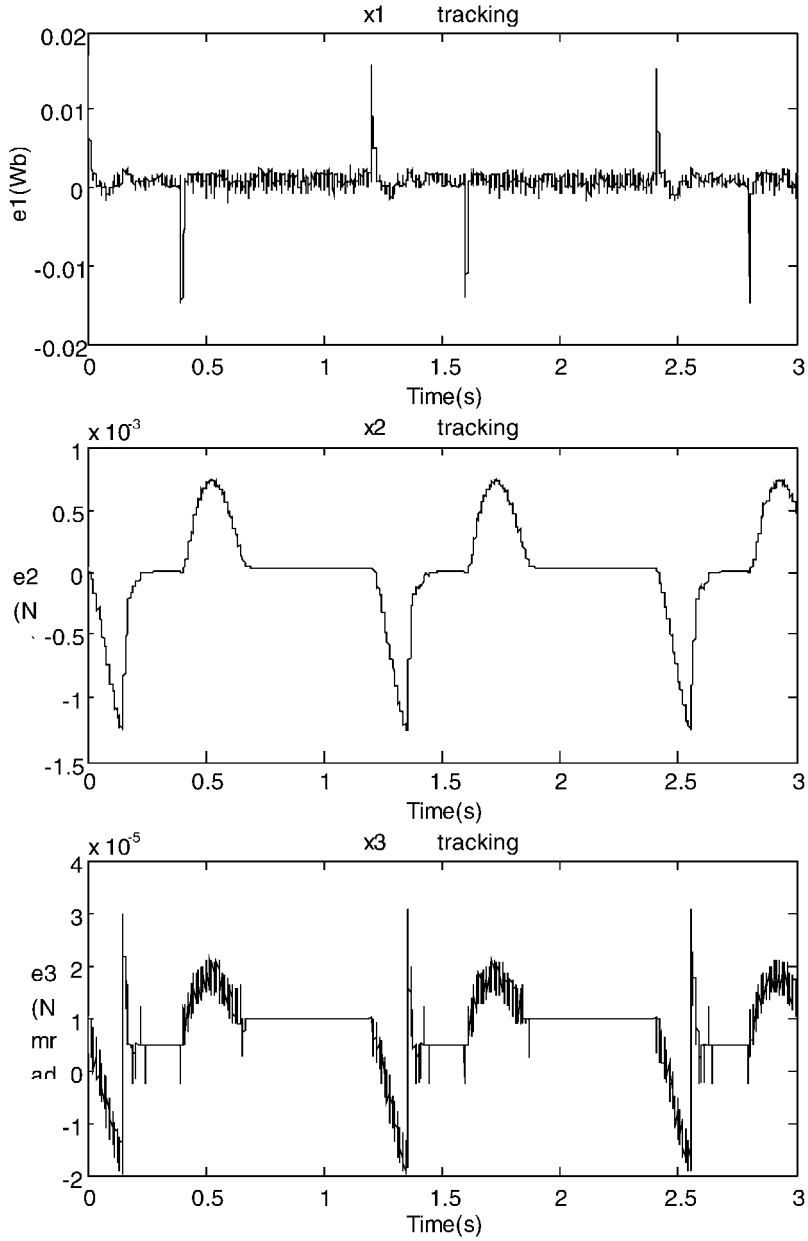

Fig. 9 Experimental results for the tracking error of each state with damping injection

China (60174025) and the Hong Kong Polytechnic University through Research Project G-V777.

REFERENCES

1 **Du, K. H., Su, C., Lim, M. K.** and **Jin, W. L.** A micromachined thermally-driven gripper: a numerical and experimental study. *Smart Mater. Struct.*, 1999, **8**, 616–622.

2 **Caldwell, D. G.** and **Tsagarakis, N.** 'Soft' grasping using a dextrous hand. *Industrial Robot: An Int. J.*, 2000, **27**(3), 194–199.

3 **Lorenz, R. D., Zik, J. J.** and **Sykora, D. J.** A direct-drive, robot parts, and tooling gripper with high-performance force feedback control. *IEEE Trans. Ind. Applic.*, 1991, **27**(2), 275–281.

4 **Monkman, G.** Precise piezoelectric prehension. *Industrial Robot: An Int. J.*, 2000, **27**(3), 189–193.

5 **Chan, K.** and **Cheung, N. C.** Modelling and characterisation of high performance variable reluctance finger gripper. In International Power Engineering Conference (*IPEC 2001*), Singapore, 17–19 May 2001, Vol. 1, pp. 370–375.

6 **Miller, T. J. E.** *Switched Reluctance Motors and their Control*, 1993 (Magne Physical Publishing and Clarendon Press, Oxford).

7 **Ilic'-Spong, M., Marino, R., Peresada, S. M.** and **Taylor, D.** Feedback linearizing control of switched reluctance motors. *IEEE Trans. Autom. Control*, 1987, **32**(5), 371–379.

8 **Amor, L. B.** and **Dessaint. L.-A.** Adaptive feedback linearization for position control of a switched reluctance motor: analysis and simulation. *Int. J. Adaptive Control and Signal Processing*, 1993, **7**(2), 117–136.

9 **Bortoff, S. A., Kohan, R. R.** and **Milman, R.** Adaptive

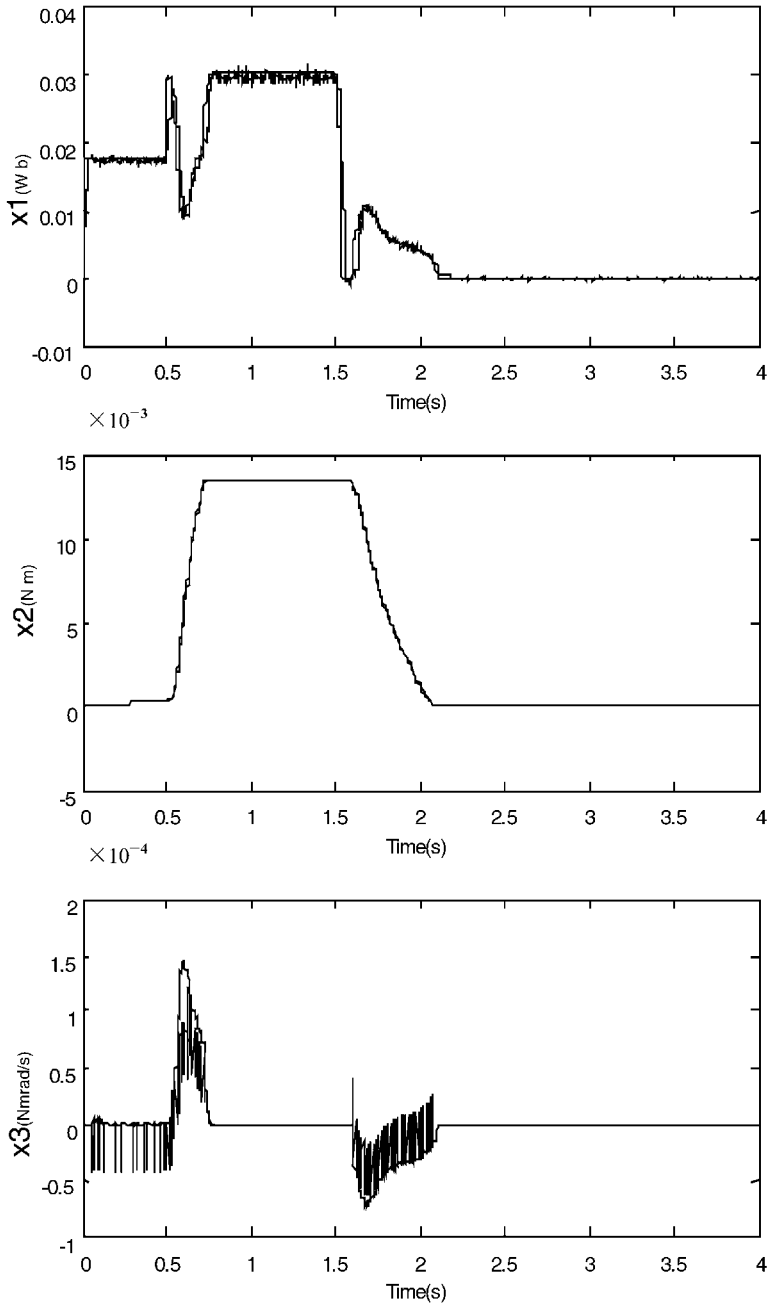

Fig. 10 Experimental result of the PBC combined with trajectory planning

control of variable reluctance motors: a spline function approach. *IEEE Trans. Ind. Electronics*, 1998, **45**(3), 433–444.

10 **Ortega, R.** and **Van Der Schaft, A.** Putting energy back in control. *IEEE Control Syst. Mag.*, 2001, **21**(2), 18–33.

11 **Fliess, M., Levine, J., Martin, P.** and **Rouchon, P.** Design of trajectory stabilizing feedback for driftless flat system. In Proceedings of the 3rd European Control Conference, Rome, Italy, 5–8 September 1995, pp. 1882–1887.

12 **Amor, L. B., Dessaint, L. A.** and **Akhrif, O.** Adaptive nonlinear torque control of a switched reluctance motor via flux observation. *Math. and Computers in Simulation*, 1995, **38**, 345–358.

13 **Angulo-Nunez, M. I.** and **Sira-Ramirez, H.** Flatness in the passivity based control of DC-to-DC power converters. In Proceedings of the 37th IEEE Conference on *Decision and Control*, Tampa, Florida, 16–18 December 1998, pp. 4115–4120.

14 **Sira-Ramirez, H.** Trajectory planning in the regulation of a PM stepper motor: a combined passivity and flatness approach. In Proceedings of the American Control Conference, Chicago, Illinois, 28–30 January 2000, pp. 1088–1092.